

Supporting Information for

Design and Engineering of Neuroglobin to Catalyze the Synthesis of Indigo and Derivatives for Textile Dyeing

Lei Chen ^{a,‡}, Jia-Kun Xu ^{b,‡}, Lianzhi Li ^c, Shu-Qin Gao ^d, Ge-Bo Wen ^d, and Ying-Wu
Lin ^{a,d*}

^a School of Chemistry and Chemical Engineering, University of South China, Hengyang 421001,
China;

^b Key Lab of Sustainable Development of Polar Fisheries, Yellow Sea Fisheries Research Institute,
Chinese Academy of Fishery Sciences, Qingdao 266071, China;

^c School of Chemistry and Chemical Engineering, Liaocheng University, Liaocheng 252059,
China;

^d Lab of Protein Structure and Function, University of South China, Hengyang 421001, China.

[‡]These authors contributed equally.

Corresponding authors:

E-mail address: ywlin@usc.edu.cn

Contents

- 1. Figure S1** ESI-MS spectra of A15C/H64D/F49Y Ngb. pS4
- 2. Figure S2** UV-Vis spectra of A15C/H64D/F49Y Ngb. pS4
- 3. Figure S3** Stopped-flow spectra of ferric A15C/H64D/F49Y Ngb in the reaction with H₂O₂ or *m*-CPBA. pS5
- 4. Figure S4** Procedure for re-dissolving the product in DMF, and the UV-Vis spectra. pS6
- 5. Figure S5** ESI-MS spectra of the oxidation product of indole in precipitation catalyzed by A15C/H64D/F49Y Ngb. pS7
- 6. Figure S6** Solution color and UV-Vis spectral changes of the oxidation of indole catalyzed by WT Ngb. pS7
- 7. Figure S7** HPCL trace of indole and the calibration curve. pS8
- 8. Figure S8** HPLC analysis of the liquid supernatant and the precipitation of the reaction catalyzed by A15C/H64D/F49Y Ngb and A15C/H64D Ngb. pS9
- 9. Figure S9** Solution color and UV-Vis spectral changes of the oxidation of indole derivatives catalyzed by the A15C/H64D/F49Y Ngb. pS10
- 10. Figure S10** ESI-MS of the oxidation products of indole derivatives as catalyzed by A15C/H64D/F49Y Ngb. pS12
- 11. Figure S11** HPLC analysis of authentic samples of indole derivatives and oxidation products catalyzed by A15C/H64D/F49Y Ngb. pS13
- 12. Figure S12** Molecular docking structures of 5-chloroindole, 6-chloroindole, 7-chloroindole, 6-bromoindole, and 5-nitroindole in complex with A15C/H64D/F49Y Ngb. pS16
- 13. Figure S13** Solution color of 4,4'-dichloroindigo and 4,4'-dinitroindigo and that mixed in the volume of 1:1 and 2:1, respectively. pS17

- 14. Figure S14** Chemical reaction and ESI-MS of the oxidation products of co-substrates containing 4-chloroindole and 4-nitroindole catalyzed by A15C/H64D/F49Y Ngb. pS17
- 15. Table S1** The amounts of indigo, side products and unreacted indole after reaction catalyzed by Ngb mutants, and determined by HPLC. pS18
- 16. Table S2** Docking energy of indole binding to A15C/H64D/F49Y Ngb. pS19
- 17. Table S3** Docking energy of 4-chloroindole binding to A15C/H64D/F49Y Ngb. pS19
- 18. Table S4** Docking energy of 5-chloroindole binding to A15C/H64D/F49Y Ngb. pS20
- 19. Table S5** Docking energy of 6-chloroindole binding to A15C/H64D/F49Y Ngb. pS20
- 20. Table S6** Docking energy of 7-chloroindole binding to A15C/H64D/F49Y Ngb. pS21
- 21. Table S7** Docking energy of 4-nitroindole binding to A15C/H64D/F49Y Ngb. pS21
- 22. Table S8** Docking energy of 5-nitroindole binding to A15C/H64D/F49Y Ngb. pS22
- 23. Table S9** Docking energy of 6-bromoindole binding to A15C/H64D/F49Y Ngb. pS22

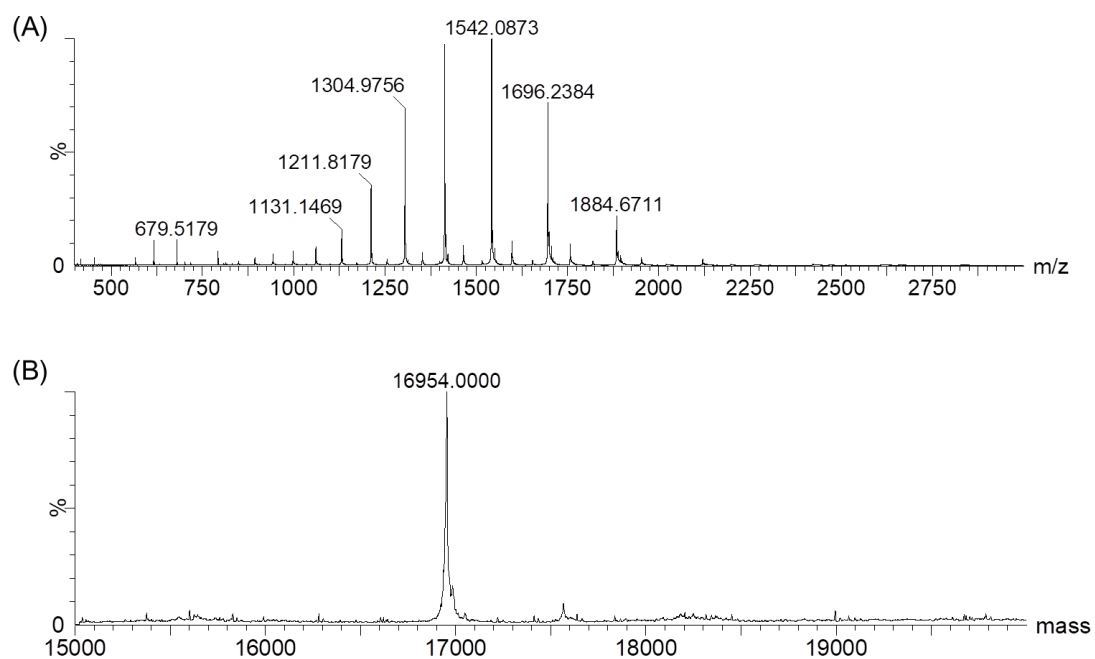


Figure S1. ESI-MS spectrum of A15C/H64D/F49Y Ngb. (A) The multiply-charged peaks, and (B) the observed mass 16954 Da (calculated apo-protein without formation of two disulfide bonds: 16959 Da).

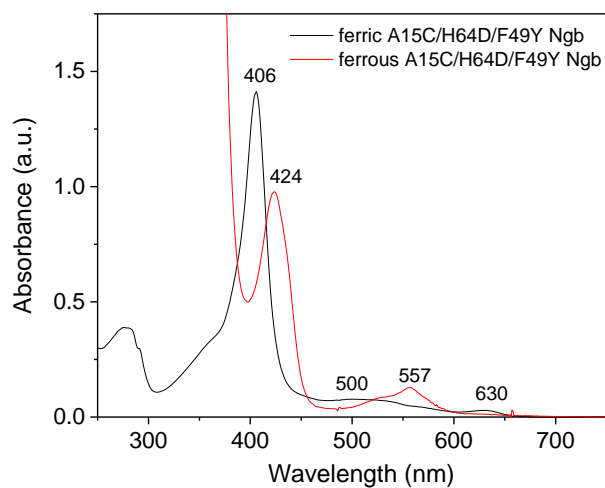


Figure S2. UV-Vis spectra of A15C/H64D/F49Y Ngb (10 μ M) in ferric (black) and ferrous (red) forms.

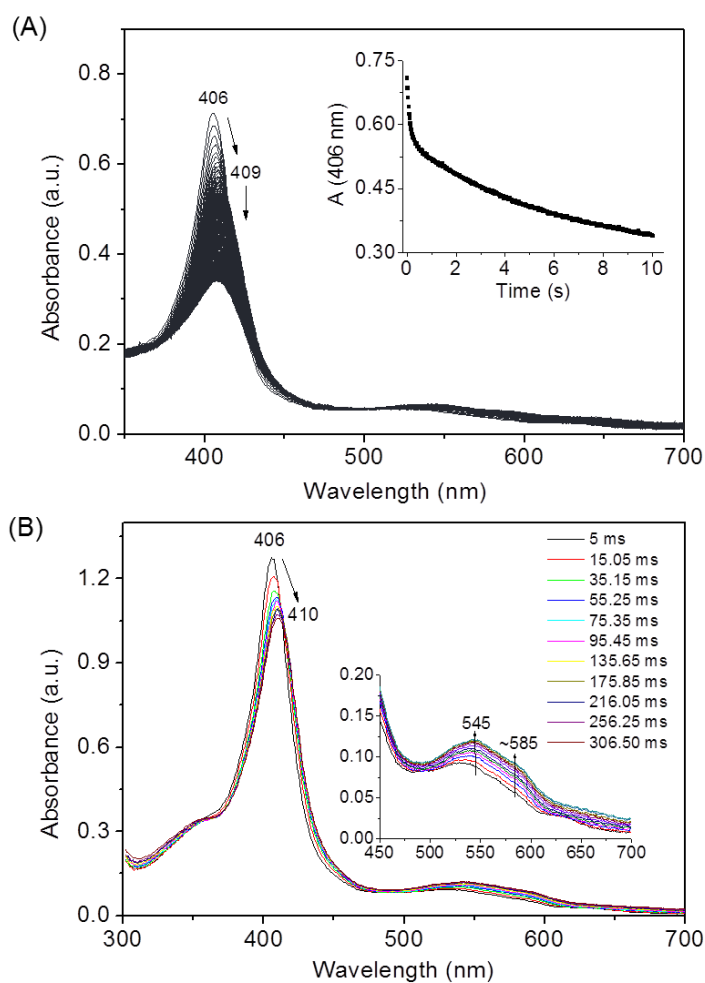


Figure S3. Stopped-flow spectra of ferric A15C/H64D/F49Y Ngb in the reaction with (A) H_2O_2 (1 mM) at pH 6.0 for 10 sec, and the inset shows the decay of Soret band at 406 nm over time, and (B) *m*-CPBA (0.1 mM) at pH 6.0 for ~0.3 sec. The inset shows the changes of the visible bands.

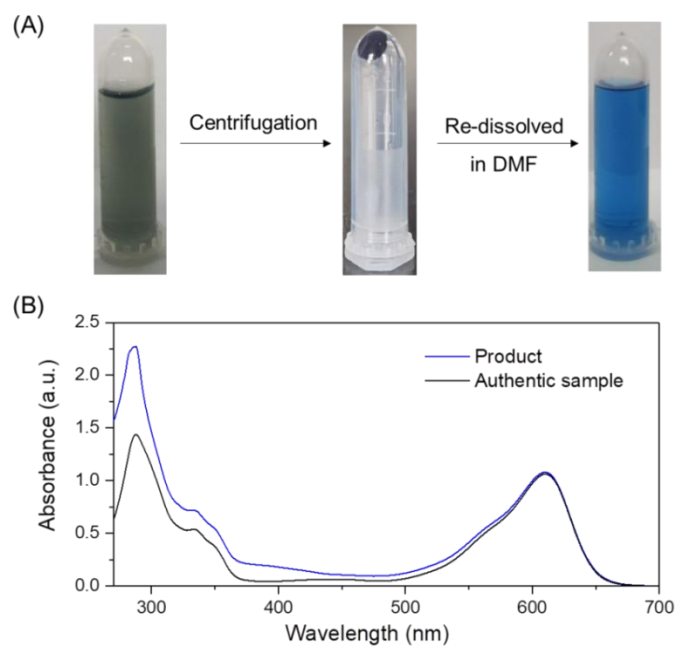


Figure S4. (A) Procedure for re-dissolving the product in DMF. The reaction solution of indole, as catalyzed by A15C/H64D/F49Y Ngb, produced blue precipitates after centrifugation, which generated a transparent blue solution by re-dissolving in DMF. (B) UV-Vis spectra of the biosynthesized indigo (blue) and the authentic indigo sample (black) in DMF.

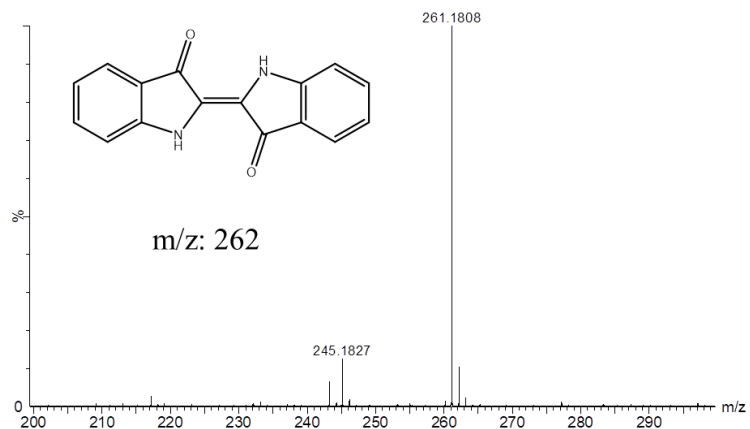


Figure S5. ESI-MS spectra of the oxidation product of indole in precipitation catalyzed by A15C/H64D/F49Y Ngb. Indigo ($C_{16}H_{10}N_2O_2$), Calculated: 262.1 Da; Observed: 261.18 Da ($[M-H]^-$).

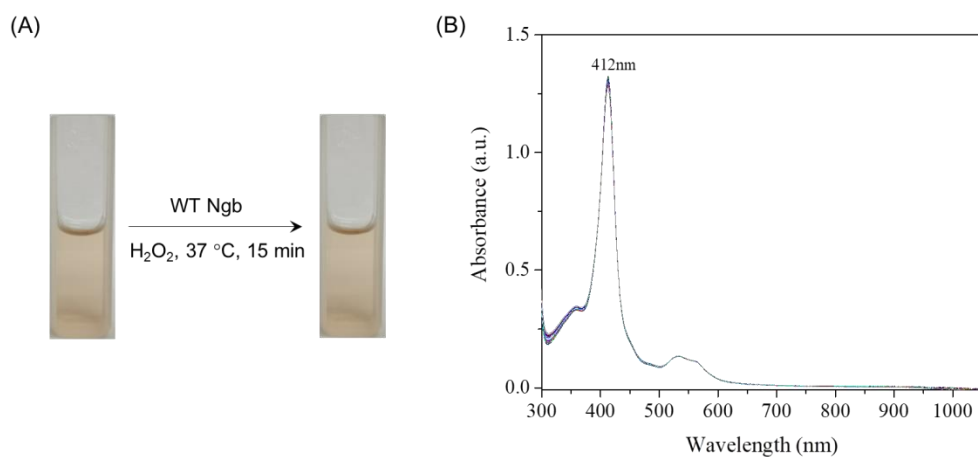


Figure S6. (A) Solution color of the oxidation of indole (1 mM) catalyzed by WT Ngb (10 μ M) with H_2O_2 (1 mM) as an oxidant. (B) UV-Vis spectral changes upon the oxidation of indole catalyzed by WT Ngb.

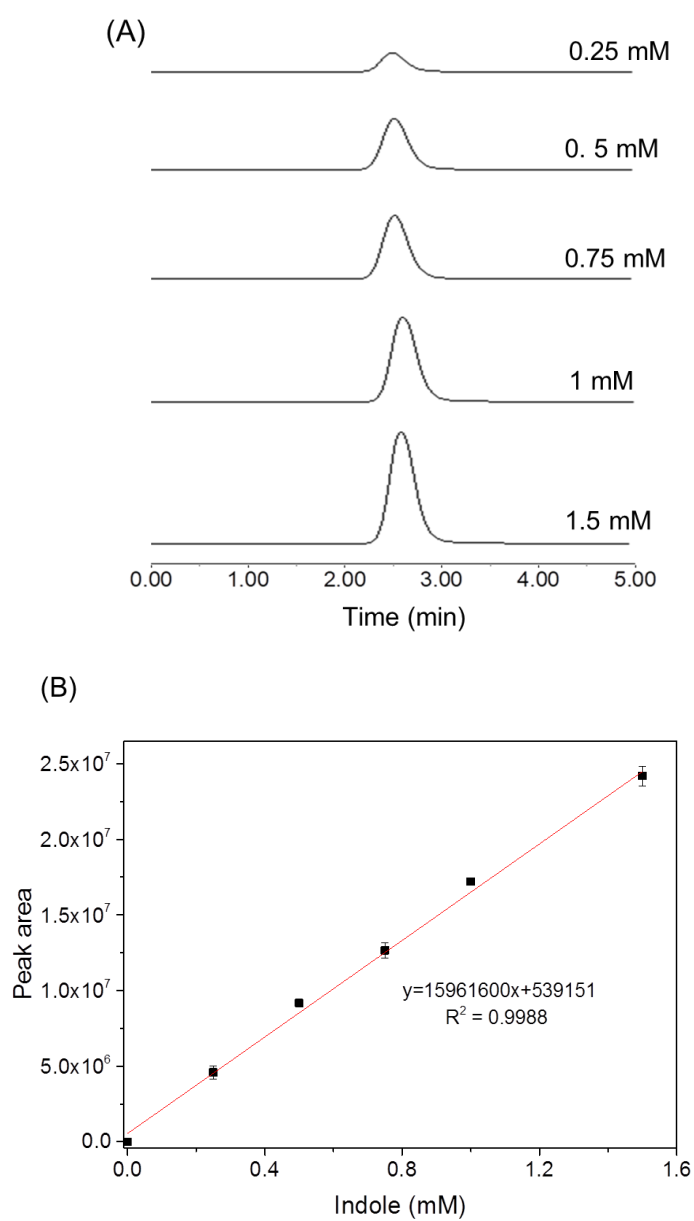


Figure S7. HPLC trace of indole (A) and the calibration curve (B).

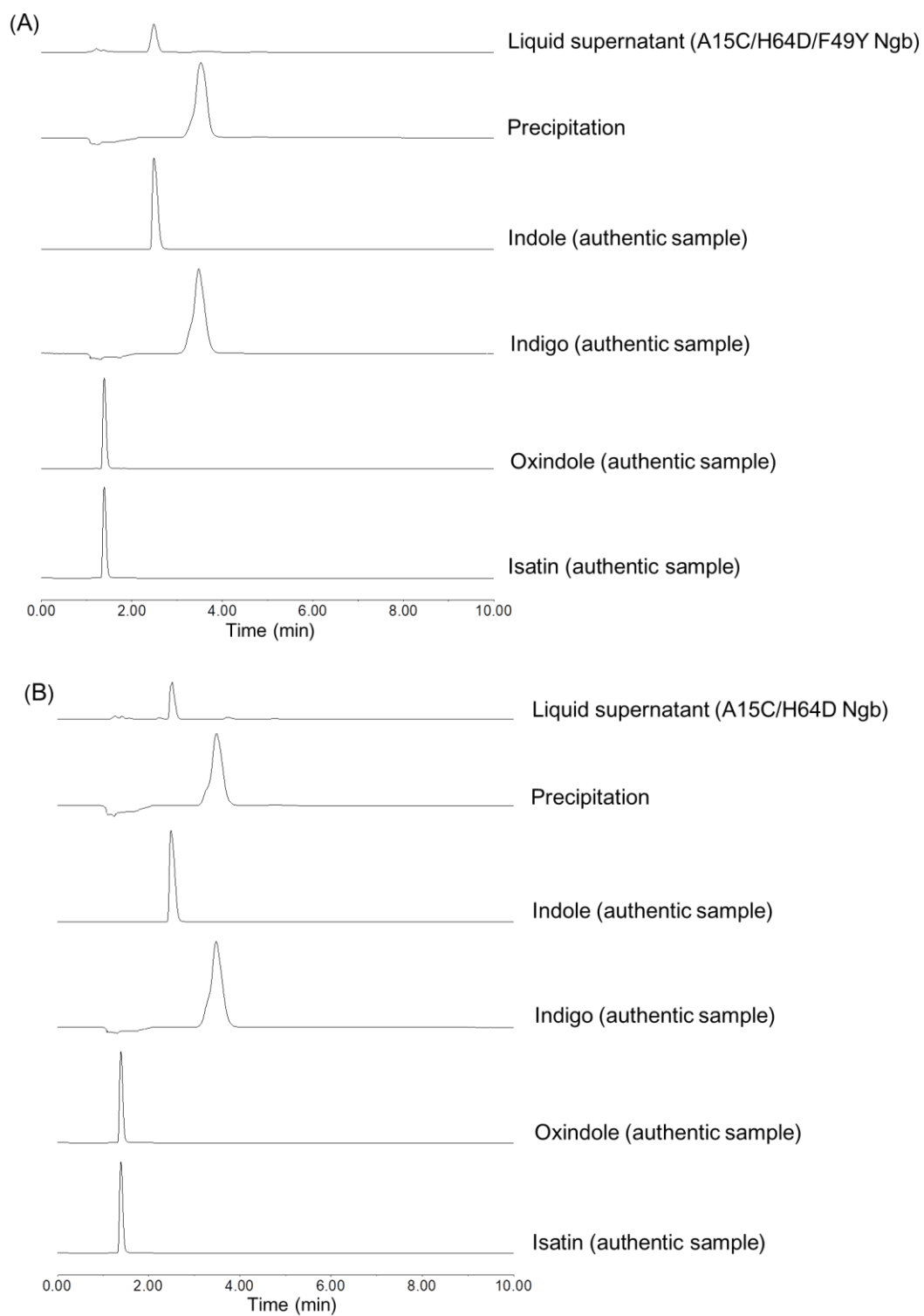
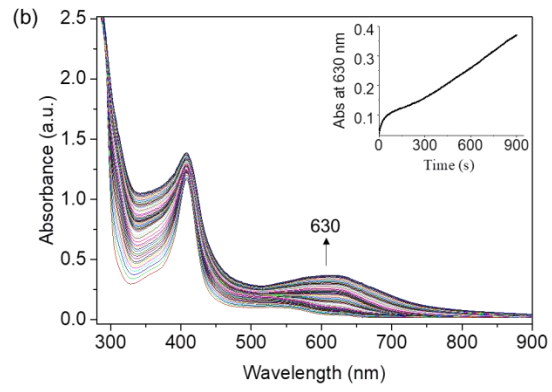
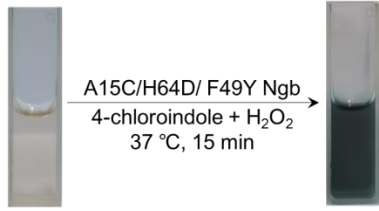
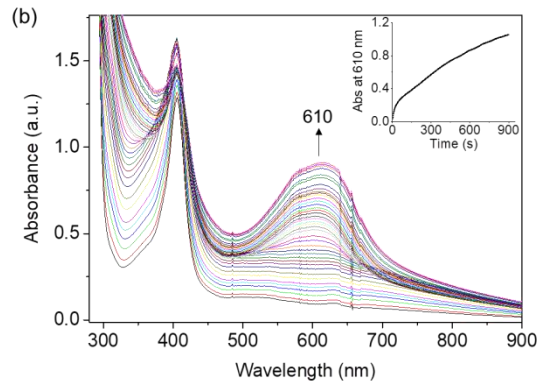
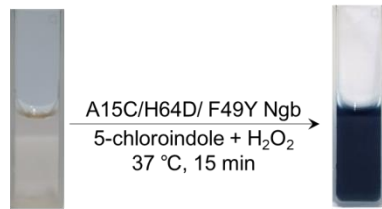


Figure S8. HPLC analysis of the extraction from the liquid supernatant and the precipitation of the reaction monitored at 280 nm, as catalyzed by A15C/H64D/F49Y Ngb (A) and A15C/H64D Ngb (B), respectively. HPLC traces of authentic samples of oxindole, isatin and indigo were shown for comparison.

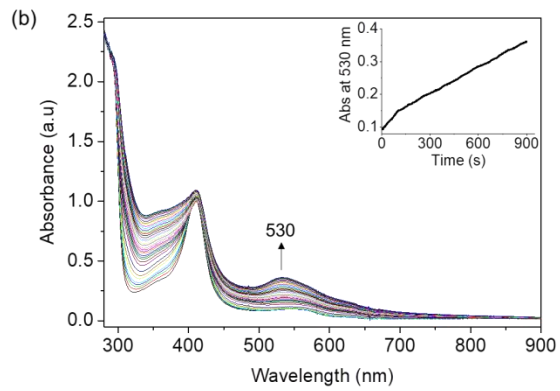
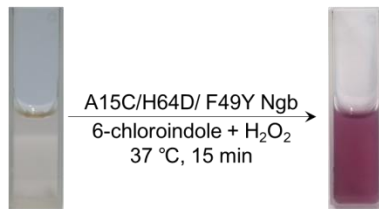
(A) (a)



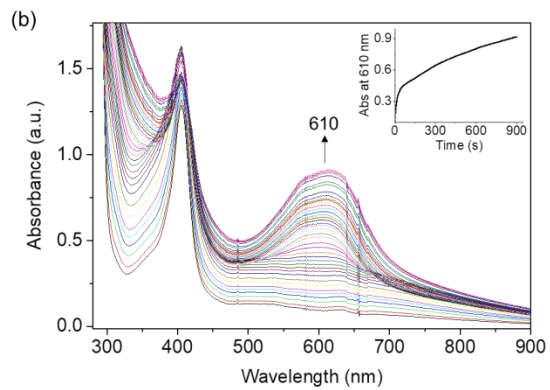
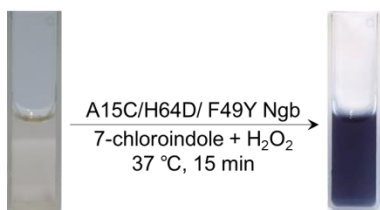
(B) (a)



(C) (a)



(D) (a)



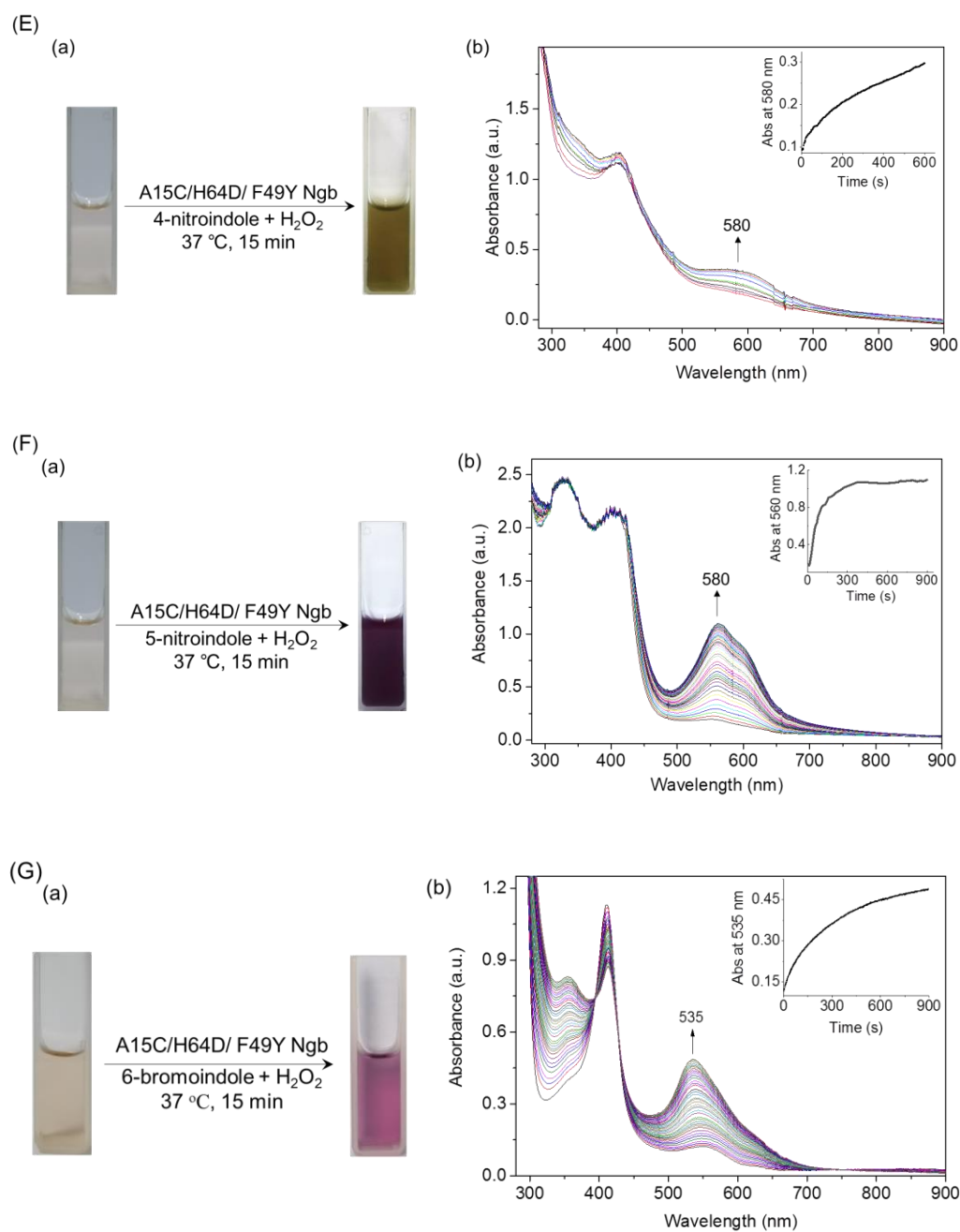
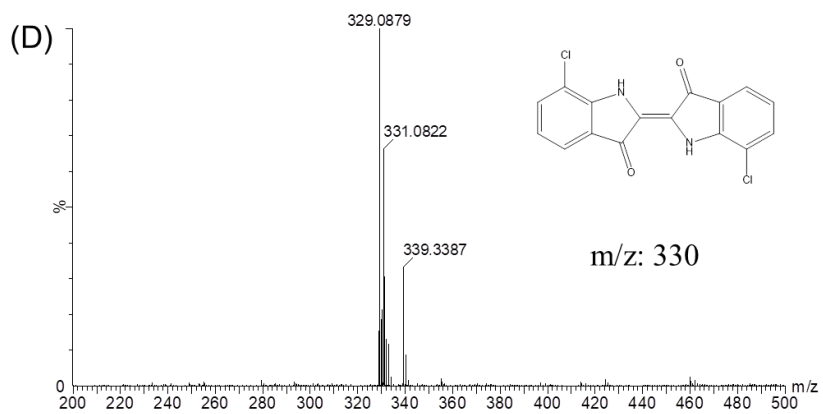
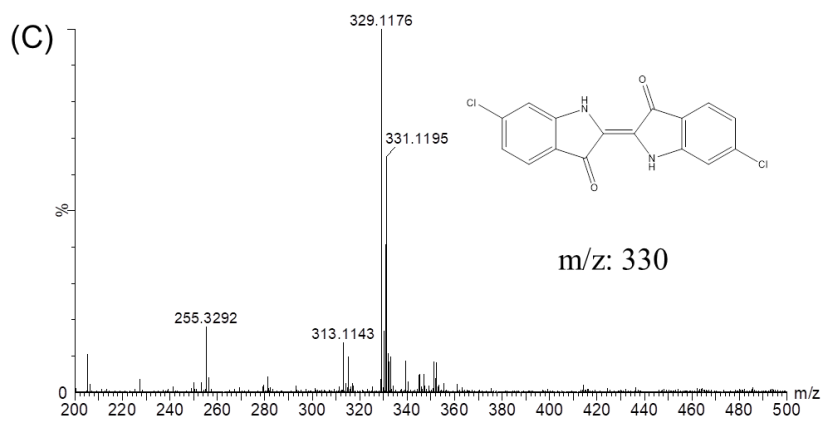
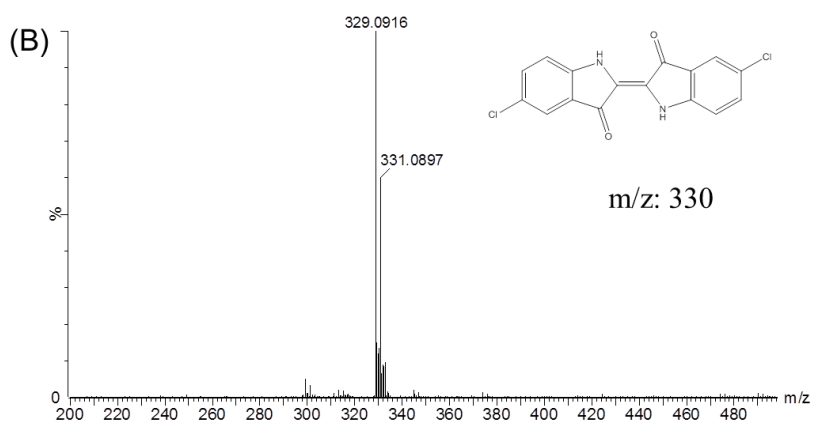
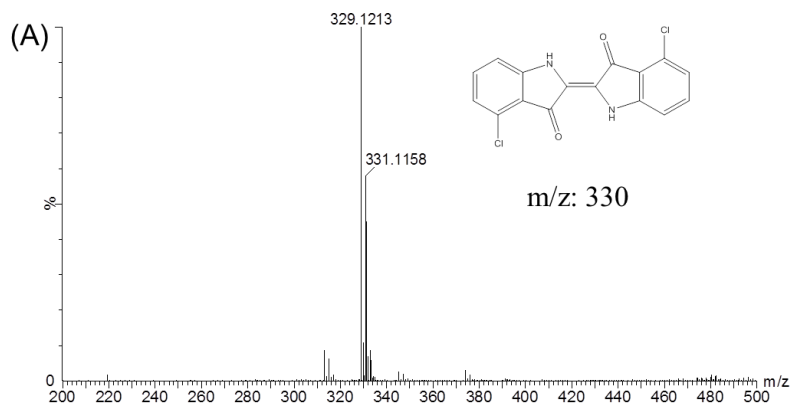


Figure S9. The solution color (a) and UV-Vis spectral changes (b) of the oxidation of indole derivatives (1 mM) catalyzed by the A15C/H64D/F49Y Ngb (10 μM) in 50 mM potassium phosphate buffer (pH 7.0), with 1 mM H_2O_2 in a final volume of 2 mL. The reaction was performed at 37 $^\circ\text{C}$ for 15 min. (A) 4-chloroindole, (B) 5-chloroindole, (C) 6-chloroindole, (D) 7-chloroindole, (E) 4-nitroindole, (F) 5-nitroindole and (G) 6-bromoindole.



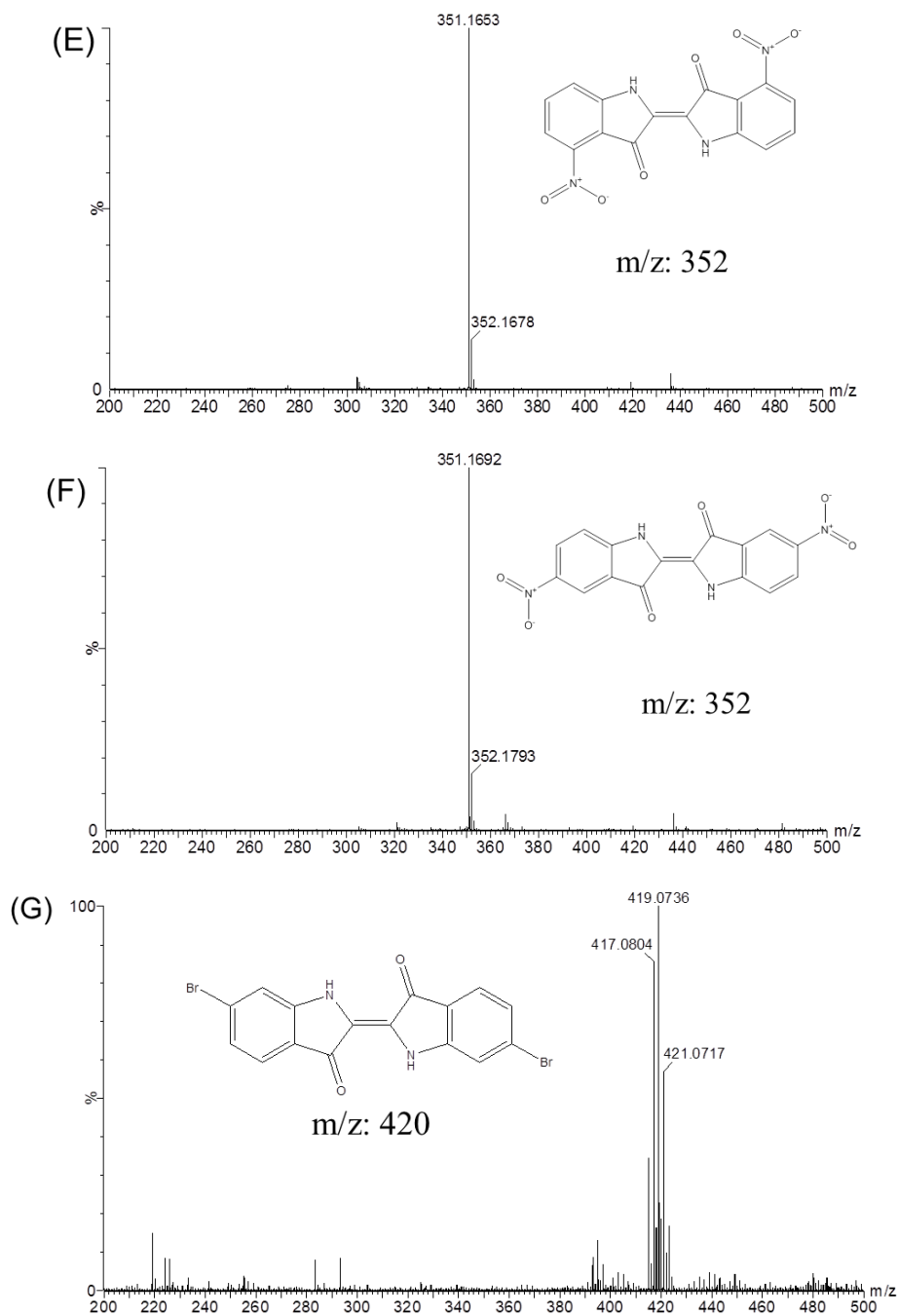
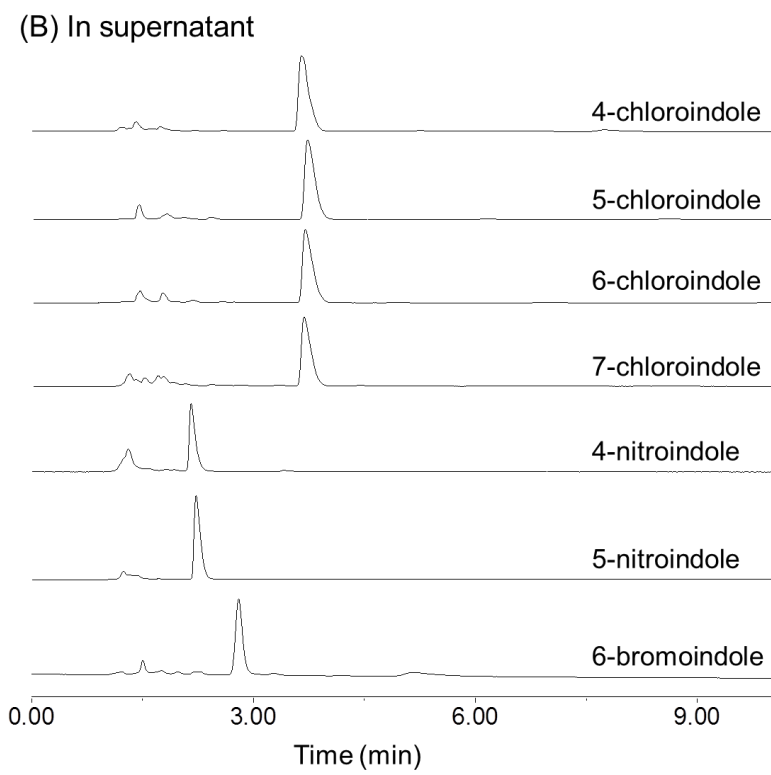
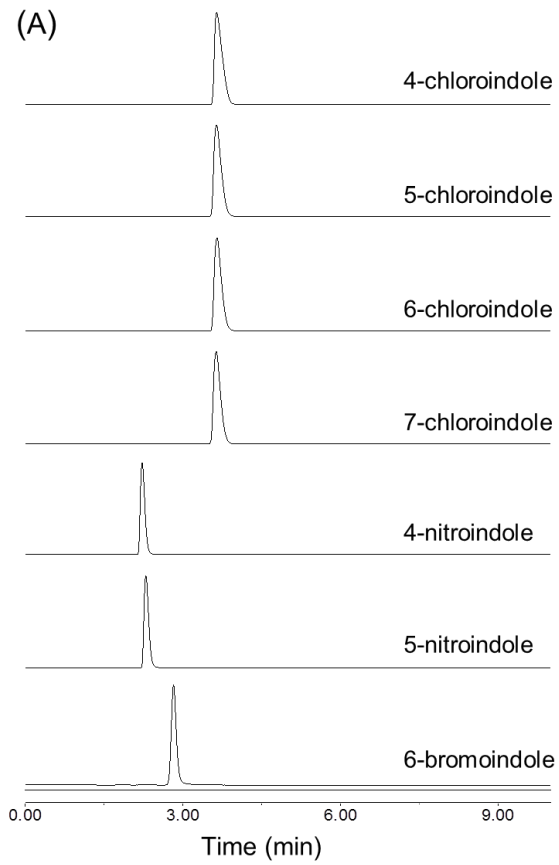


Figure S10. ESI-MS of the oxidation products of indole derivatives, 4-chloroindole (A), 5-chloroindole (B), 6-chloroindole (C), 7-chloroindole (D), 4-nitroindole (E), 5-nitroindole (F) and 6-bromoindole (G), as catalyzed by A15C/H64D/F49Y Ngb.



(C) In precipitation

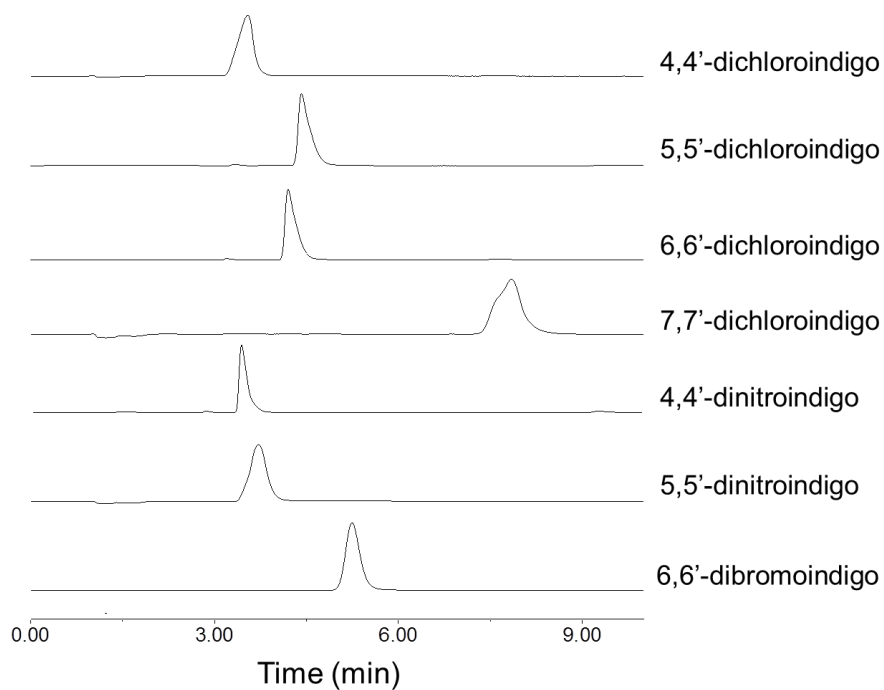


Figure S11. (A) HPLC traces of authentic samples of 4-chloroindole, 5-chloroindole, 6-chloroindole, 7-chloroindole, 4-nitroindole, 5-nitroindole and 6-bromoindole, monitored at 280 nm. HPLC analysis of the reaction products in liquid supernatant (B) and precipitation (C) monitored at 280 nm, as catalyzed by A15C/H64D/F49Y Ngb.

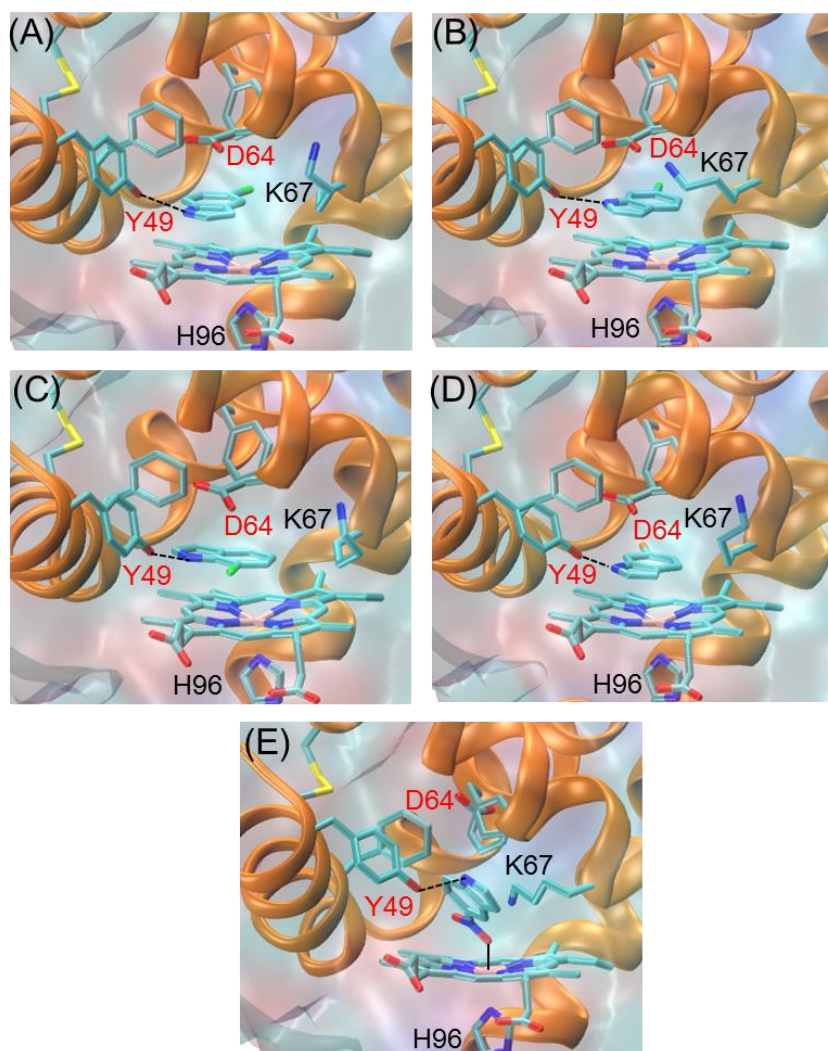


Figure S12. Molecular docking structures of (A) 5-chloroindole, (B) 6-chloroindole, (C) 7-chloroindole, (D) 6-bromoindole, and (E) 5-nitroindole in complex with A15C/H64D/F49Y Ngb. The disulfide bond and the heme active were highlighted. The H-bond and coordination interactions are indicated by dashed and solid lines, respectively.

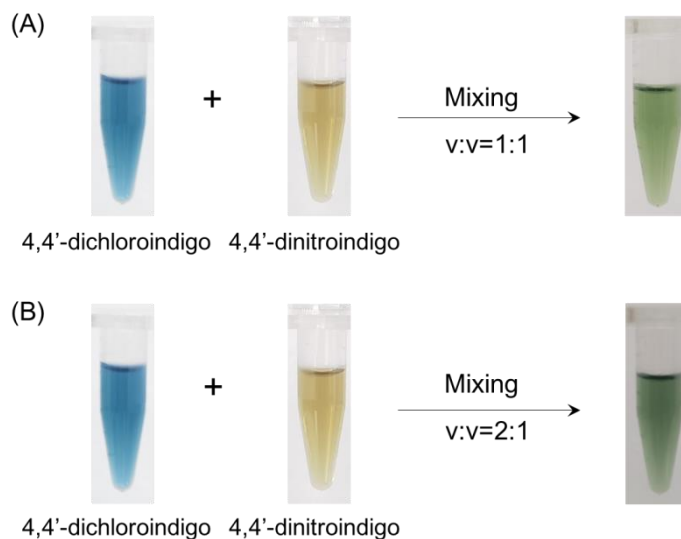


Figure S13. Solution color of 4,4'-dichloroindigo and 4,4'-dinitroindigo catalyzed by A15C/H64D/F49Y Ngb (10 μ M) with the substrate (1 mM), H₂O₂ (1 mM), at 37 °C for 15 min, and that after mixed in the volume of 1:1 (A) and 2:1 (B), respectively.

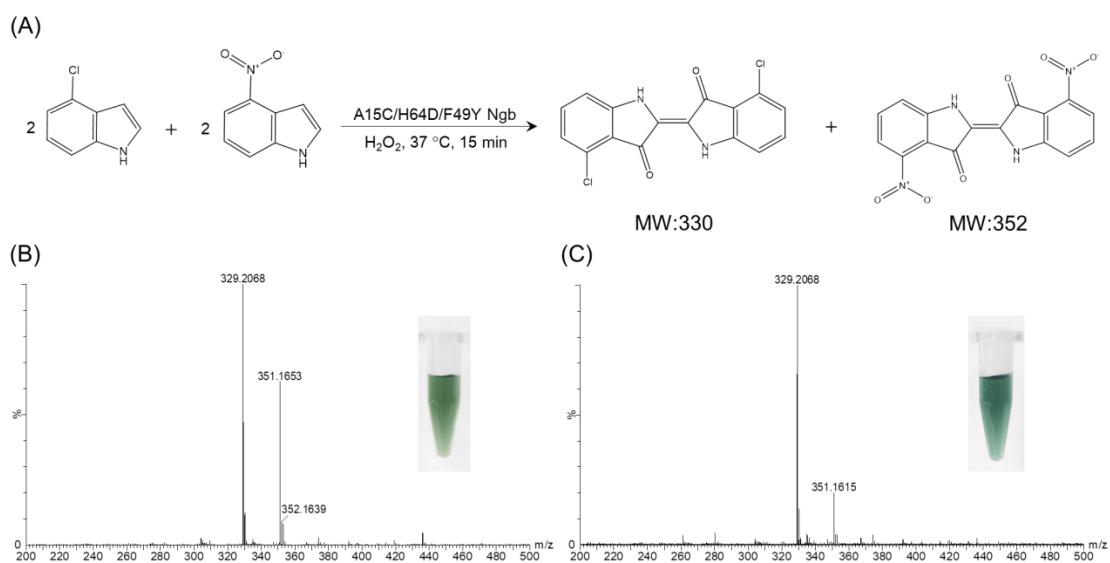


Figure S14. Chemical reaction (A) and ESI-MS of the oxidation products of co-substrates (2 mM) containing 4-chloroindole and 4-nitroindole (B, a mole ratio of 1 to 1; C, a mole ratio of 1 to 1), as catalyzed by A15C/H64D/F49Y Ngb (10 μ M), 1 mM H₂O₂ in 50 mM potassium phosphate buffer (pH 7.0) at 37 °C for 15 min. The digital photos of the solution after reaction were shown as insets.

Table S1. The amounts of indigo, side products and unreacted indole after reaction, as catalyzed by Ngb mutants and determined by HPLC, with those of Mb mutants shown for comparison.

Protein	Indigo (μM)	Oxindole (μM)	Isatin (μM)	Indole (μM)	Other areas	Indigo yield
A15C/H64D Ngb	288	15	40	177	0.54	70%
A15C/H64D/F49Y Ngb	340	10	64	167	0.32	82%
F43Y Mb ^(a)	180	31	59	332	0.021	54%
H64D Mb ^(b)	36	21	34	643	0.16	20%
F43Y/H64D Mb ^(a)	120	10	60	292	0.084	34%
H64D/V68I/I107V Mb ^(b)	34	31	46	448	0.18	11%

(a) Liu *et al.* *RSC Adv.* **2018**, 8, 33325–33330.

(b) Xu *et al.* *Catal. Sci. Technol.* **2012**, 2, 739–744.

Table S2. Docking energy of indole binding to A15C/H64D/F49Y Ngb.

Model	$E_{\text{binding}}^{\text{a}}$	$E_{\text{inter-mol}}^{\text{b}}$	$E_{\text{vdw}}^{\text{c}}$	$E_{\text{elec}}^{\text{d}}$
1	-5.82	-5.82	-1.54	0.08
2	-5.70	-5.70	-1.09	0.00
3	-5.69	-5.69	-1.51	0.08
4	-5.67	-5.67	-1.04	0.06
5	-5.67	-5.67	-1.22	0.06
6	-5.66	-5.66	-1.32	0.01
7	-5.64	-5.64	-1.07	0.03
8	-5.64	-5.64	-1.06	0.03
9	-5.63	-5.63	-1.53	0.04
10	-5.63	-5.63	-1.54	0.04

^a Binding energy. ^b Intermolecular energy. ^c van der Waals energies. ^d Electrostatic interactions. Unit: kcal/mol.

Table S3. Docking energy of 4-chloroindole binding to A15C/H64D/F49Y Ngb.

Model	$E_{\text{binding}}^{\text{a}}$	$E_{\text{inter-mol}}^{\text{b}}$	$E_{\text{vdw}}^{\text{c}}$	$E_{\text{elec}}^{\text{d}}$
1	-6.64	-6.64	-2.21	-0.02
2	-6.64	-6.64	-1.77	0.05
3	-6.57	-6.57	-1.73	0.04
4	-6.57	-6.57	-1.90	0.03
5	-6.56	-6.56	-1.60	0.02
6	-6.49	-6.49	-2.05	-0.03
7	-6.49	-6.49	-1.70	0.04
8	-6.48	-6.48	-1.57	0.01
9	-6.45	-6.45	-1.67	0.00
10	-6.44	-6.44	-2.02	-0.02

^a Binding energy. ^b Intermolecular energy. ^c van der Waals energies. ^d Electrostatic interactions. Unit: kcal/mol.

Table S4. Docking energy of 5-chloroindole binding to A15C/H64D/F49Y Ngb.

Model	E_{binding}^a	$E_{\text{inter-mol}}^b$	E_{vdw}^c	E_{elec}^d
1	-6.93	-6.93	-2.28	-0.06
2	-6.48	-6.48	-1.76	0.02
3	-6.48	-6.48	-1.71	0.02
4	-6.38	-6.38	-1.65	-0.01
5	-6.37	-6.37	-1.67	0.02
6	-6.36	-6.36	-1.71	0.01
7	-6.35	-6.35	-1.58	-0.02
8	-6.33	-6.33	-1.63	0.01
9	-6.32	-6.32	-1.80	-0.01
10	-6.30	-6.30	-1.58	-0.01

^a Binding energy. ^b Intermolecular energy. ^c van der Waals energies. ^d Electrostatic interactions. Unit: kcal/mol.

Table S5. Docking energy of 6-chloroindole binding to A15C/H64D/F49Y Ngb.

Model	E_{binding}^a	$E_{\text{inter-mol}}^b$	E_{vdw}^c	E_{elec}^d
1	-6.50	-6.50	-1.83	0.10
2	-6.49	-6.49	-1.69	0.06
3	-6.36	-6.36	-1.65	0.08
4	-6.36	-6.36	-1.56	0.07
5	-6.31	-6.31	-1.66	0.09
6	-6.31	-6.31	-1.63	0.04
7	-6.29	-6.29	-1.40	0.02
8	-6.24	-6.24	-1.42	0.01
9	-6.23	-6.23	-1.11	-0.03
10	-6.21	-6.21	-1.45	0.01

^a Binding energy. ^b Intermolecular energy. ^c van der Waals energies. ^d Electrostatic interactions. Unit: kcal/mol.

Table S6. Docking energy of 7-chloroindole binding to A15C/H64D/F49Y Ngb.

Model	$E_{\text{binding}}^{\text{a}}$	$E_{\text{inter-mol}}^{\text{b}}$	$E_{\text{vdw}}^{\text{c}}$	$E_{\text{elec}}^{\text{d}}$
1	-6.37	-6.37	-2.08	0.04
2	-6.32	-6.32	-1.77	0.08
3	-6.31	-6.31	-1.64	0.02
4	-6.25	-6.25	-1.82	0.04
5	-6.23	-6.23	-1.48	-0.03
6	-6.20	-6.20	-1.76	0.05
7	-6.20	-6.20	-1.56	0.01
8	-6.18	-6.18	-1.10	0.00
9	-6.18	-6.18	-1.75	0.01
10	-6.15	-6.15	-1.41	-0.04

^a Binding energy. ^b Intermolecular energy. ^c van der Waals energies. ^d Electrostatic interactions. Unit: kcal/mol.

Table S7. Docking energy of 4-nitroindole binding to A15C/H64D/F49Y Ngb.

Model	$E_{\text{binding}}^{\text{a}}$	$E_{\text{inter-mol}}^{\text{b}}$	$E_{\text{vdw}}^{\text{c}}$	$E_{\text{elec}}^{\text{d}}$
1	-13.89	-14.19	-3.31	-1.79
2	-13.35	-14.65	-2.25	-0.36
3	-13.13	-13.43	-2.08	-0.07
4	-13.05	-13.35	-1.85	-0.18
5	-13.03	-13.32	-1.72	-0.07
6	-13.02	-13.32	-1.81	-0.06
7	-13.01	-13.31	-1.83	-0.06
8	-13.00	-13.29	-2.03	-0.09
9	-13.00	-13.30	-1.68	-0.08
10	-12.97	-13.27	-2.21	-0.15

^a Binding energy. ^b Intermolecular energy. ^c van der Waals energies. ^d Electrostatic interactions. Unit: kcal/mol.

Table S8. Docking energy of 5-nitroindole binding to A15C/H64D/F49Y Ngb.

Model	$E_{\text{binding}}^{\text{a}}$	$E_{\text{inter-mol}}^{\text{b}}$	$E_{\text{vdw}}^{\text{c}}$	$E_{\text{elec}}^{\text{d}}$
1	-13.01	-13.31	-3.09	-1.50
2	-12.69	-12.99	-2.32	-1.13
3	-12.50	-12.80	-2.05	-1.01
4	-12.39	-12.69	-1.89	-1.09
5	-12.37	-12.67	-2.12	-1.13
6	-12.08	-12.37	-2.40	-1.09
7	-12.07	-12.37	-1.91	-0.04
8	-11.82	-12.12	-1.73	-0.03
9	-11.76	-12.06	-1.65	-0.05
10	-11.75	-12.05	-1.79	-0.18

^a Binding energy. ^b Intermolecular energy. ^c van der Waals energies. ^d Electrostatic interactions. Unit: kcal/mol.

Table S9. Docking energy of 6-bromoindole binding to A15C/H64D/F49Y Ngb.

Model	$E_{\text{binding}}^{\text{a}}$	$E_{\text{inter-mol}}^{\text{b}}$	$E_{\text{vdw}}^{\text{c}}$	$E_{\text{elec}}^{\text{d}}$
1	-7.15	-7.15	-2.34	0.03
2	-7.14	-7.14	-2.29	0.08
3	-7.14	-7.14	-2.15	0.02
4	-7.09	-7.09	-2.26	0.08
5	-7.07	-7.07	-2.20	0.03
6	-7.04	-7.04	-2.11	0.01
7	-7.04	-7.04	-2.03	-0.02
8	-7.01	-7.01	-2.14	0.01
9	-7.00	-7.00	-2.21	0.08
10	-6.99	-6.99	-2.07	0.00

^a Binding energy. ^b Intermolecular energy. ^c van der Waals energies. ^d Electrostatic interactions. Unit: kcal/mol.